

Optimization of Active Region of Quantum Cascade Laser (QCL) by Coupled Calculation of Genetic Algorithm and QCL Simulator

Shigeyuki Takagi¹^a, Tsutomu Kakuno², Rei Hashimoto², Kei Kaneko² and Shinji Saito²^b

¹*Department of Electrical and Electronics Engineering, School of Engineering, Tokyo University of Technology, 1404-1 Katakura, Hachioji, Tokyo, Japan*

²*Corporate Manufacturing Engineering Center, Toshiba Corporation, 33 Shinisogo, Isogo, Yokohama, Kanagawa, Japan*

Keywords: Quantum Cascade Lasers, QCLs, Active Region, non-Equilibrium Green's Function, Genetic Algorithm, GA, Optimization, Gain, Wavelength, Injector Barrier, Well.

Abstract: We applied a coupled calculation of genetic algorithm and a quantum cascade laser (QCL) simulator (nextnano.QCL) to calculate the gain that excites laser light in the active region of the QCL. The film thicknesses of the nine layers constituting the active region were changed simultaneously, and the film structure with the maximum gain was determined from 1000 type of film structures. The QCL simulator incorporating a non-equilibrium Green's function was used to calculate the gain of the QCL, and the validity of the simulation was evaluated using the active region structure reported in the previous paper. In the coupled calculation of the QCL simulator and genetic algorithms, we used gain as an objective function and methods of crossing, natural selection, and mutation simulating the evolutionary process of living organisms to optimize the thickness of nine films. As a result of the optimization calculation, the optimized structure had gain (78.44 cm^{-1}) higher than that (50.01 cm^{-1}) in a structure reported in a previous paper.


1 INTRODUCTION


Quantum cascade lasers (QCLs) are n-type semiconductor lasers in which two types of semiconductor film are alternately stacked, and the laser light in the infrared region can be obtained (Faist et al., 1994). Since the wavelengths of QCLs are in the infrared region, they are expected to be applied to trace gas analysis and remote gas detection (Faist et al., 2016). It is necessary to develop a laser with a wavelength suitable for measurement. With such trace substance detection and gas detection from a distance, a higher sensitivity is expected by increasing the output. Since the amount of laser absorption is measured in the detection of trace substances, it is necessary to propagate along a large optical path length. To develop such high-power lasers, it is effective to utilize a simulator that can predict the oscillation wavelength and gain.

Figure 1 shows the band structure of a QCL. It has an injector region that transports electrons and an active region consisting of several sets of barrier and

well layers to excite laser light. Laser light is emitted when electrons transition from an upper level to a lower level in a quantum well formed in well layers. In the current simulators, the Schrödinger equation is solved to calculate the wave function, and the rate equation solution method is used at the level, where the electrons undergo transition. The amount of light emitted is calculated semiclassically from the lifetimes of the upper and lower levels, and the transition probabilities between the upper and lower levels (Lu et al., 2006). Recently, a calculation method using the non-equilibrium Green's function has been proposed (Grange, 2015). In the simulator, the distribution of electron density and the transition of electrons from the upper level to the lower level can be calculated quantumly.

To increase the output of a QCL, it is necessary to increase the intensity of the laser light excited in the active region. An effective method is to use a QCL simulator to optimize the thicknesses of the barrier and well layers in the active region by increasing the laser gain. However, the active region of a typical

^a <https://orcid.org/0009-0009-6444-8748>

^b <https://orcid.org/0000-0002-1829-6482>

QCL is composed of four barrier layers and four well layers. For this reason, the main method of optimization thus far has been to fix some film thicknesses and sequentially optimize the film thickness. Otherwise, optimization was performed under certain constraints, such as reducing the thickness of all barrier layers by a certain percentage (Tanimura et al., 2022). There are few reports on methods for simultaneously optimizing all the layers in the active region.

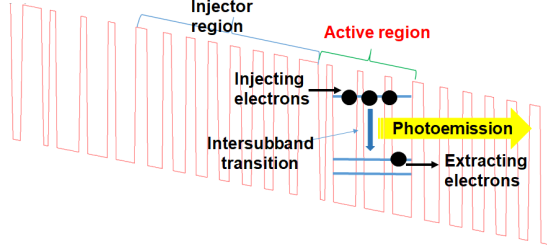


Figure 1: Band structure of QCL. (a) Injector region that transports electrons and (b) active region that excites laser light (Tanimura et al., 2022).

In this study, we developed an automatic calculation method that combines a non-equilibrium Green's function and a genetic algorithm (GA), and applied the method to optimizing the film thicknesses in the active region. Changing the thicknesses of five types of barrier layer and four types of well layers as parameters, we calculated the gain and wavelength of 1000 types of the film structures. As a result, a structure with optimized film thickness was obtained with a gain (28.43 cm^{-1}) higher than that (50.01 cm^{-1}) in the QCL structure reported in the paper. We also fabricated a prototype QCL device, performed electro-luminescence (EL) measurements, and verified the validity of the optimized results.

2 QCL SIMULATOR

2.1 QCL Simulator Incorporating non-Equilibrium Green's Function

We used nextnano.QCL (nextnano GmbH) as the QCL simulator in this study (Grange, 2015). Figure 2 shows the calculation flow in the simulator. In the Schrödinger equation, assuming that the unperturbed Hamiltonian is H_0 and the electron scattering is the perturbed Hamiltonian H_{scatt} , the Hamiltonian H in the Schrödinger as

$$H = H_0 + H_{SCATT} \quad (1)$$

Using this Hamiltonian, we solved the Schrödinger equation and calculated the electron orbit.

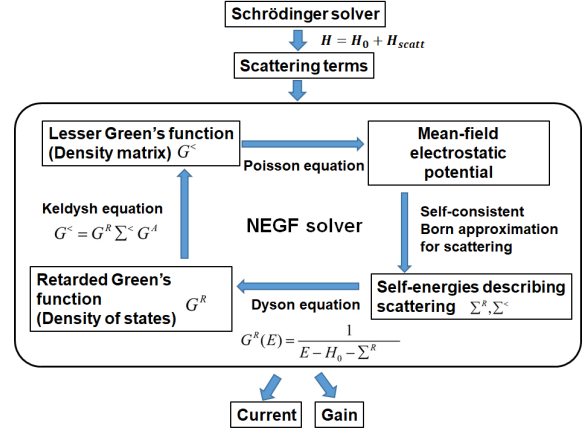


Figure 2: QCL simulator incorporating non-equilibrium Green's function (Tanimura et al., 2022).

Next, we solved Poisson's equation to find the mean-field electrostatics potential and calculated the self-energy Σ^R of delay and the self-energy $\Sigma^<$ of Lesser, which describes electron scattering. The Density of States (DOS) was obtained from the delayed Green's function G^R using the Dyson equation as follows;

$$G^R = \frac{1}{E - H_0 - \Sigma^R} \quad (2)$$

Using the Keldysh equation shown in equation (3), we calculated the electron density matrix from the Lesser Green's function $G^<$.

$$G^< = G^R \Sigma^< G^A \quad (3)$$

where G is the advanced Green's function. Current and gain were calculated based on the basis of the obtained electron density matrix.

From the calculation flow in Fig. 2, the relationship between emitted energy (wavelength) and gain was calculated. By using a non-equilibrium Green's function, we effect such as the crystal lattice and electron scattering. This is considered a major advantage over conventional semiclassical calculation methods.

2.2 Evaluation of Simulation Model

To examine the validity of this simulator, we inputted the film structure and composition reported previously into the QCL simulator (Evans et al., 2007). The film structure was modeled using two sets of injector and active regions. We assumed that the maximum gain obtained in the simulation was the laser oscillation wavelength and compared it with the oscillation

wavelength in the previous paper (Takagi et al., 2021).

Figure 3 shows the calculation results. Figure 3(a) shows the gain intensity and Fig. 3(b) shows the DOS distribution. The horizontal axes in both (a) and (b) indicate the position of the QCL film. As shown in Fig. 3(a), a high gain was observed at the position corresponding to the active region. The photon energy of this gain was 260 meV, which corresponds to a light wavelength of 4.77 nm. The oscillation wavelength obtained by Evans et al. in their experiment was 4.71 nm (Evans et al., 2007), which is in good agreement with that in our simulation.

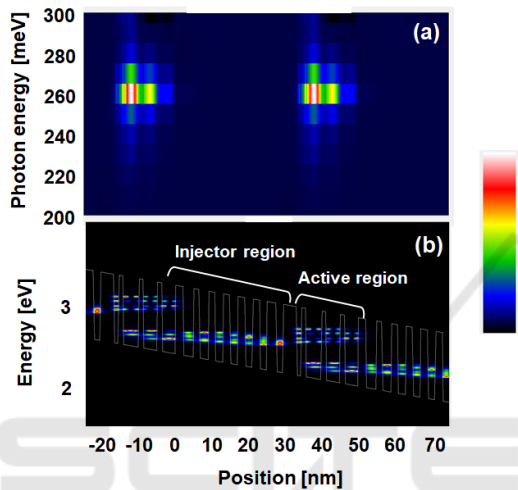


Figure 3: Calculation results of QCL simulator. (a) Gain intensity and (b) DOS.

In Fig. 3(b), there are two stages of electron distribution in the active region, and the upper and lower electron distribution regions correspond to the upper and lower levels of laser oscillation, respectively. In addition, electrons with almost the same energy level are distributed in the injector region, indicating that electrons propagated through the injector region. Nextnano.QCL was able to accurately model electron propagation and laser light emission. As a result, we were able to obtain the same calculation results for the oscillation wavelength as the experimental results.

3 COUPLED CALCULATION OF GENETIC ALGORITHMS AND QCL SIMULATOR

3.1 Optimization of Parameters

We optimized the structure of the active region that excites the laser beam shown in Fig. 4. In the active

region, the barrier layer was formed with $\text{In}_{0.363}\text{AlAs}$, and the well layer was formed with $\text{In}_{0.669}\text{GaAs}$. The thicknesses of the nine layers were optimized from the injector barrier to the fourth barrier layer. The reference structure of the active region was set to the same structure of the QCL reported by Evans et al. (Evans et al., 2007).

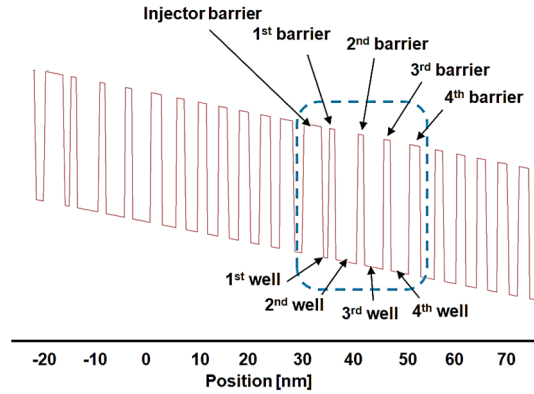


Figure 4: Optimizing film thicknesses in active region.

Table 1 shows the ranges of film thicknesses in the active region. The thickness of each film was varied within a range of ± 1.0 nm from the reference film thickness. Moreover, for films prepared by Molecular beam epitaxy (MBE), their thicknesses are less than 1.0 nm are difficult to control. Therefore, the minimum film thickness was set to 1.0 nm.

Table 1: Ranges of film thicknesses of barrier and well layers.

| Barrier/well | Film material [nm] | Thickness range [nm] | Minimum thickness [nm] |
|-------------------------|--------------------|----------------------|------------------------|
| Injector barrier | 3.8 | ± 1.0 | ≥ 1.0 |
| 1 st well | 1.2 | | |
| 1 st barrier | 1.3 | | |
| 2 nd well | 4.3 | | |
| 2 nd barrier | 1.3 | | |
| 3 rd well | 3.8 | | |
| 3 rd barrier | 1.4 | | |
| 4 th well | 3.6 | | |
| 4 th barrier | 2.2 | | |

3.2 GA and Optimization Method

To optimize the active region, we developed a calculation method that combines nextnano.QCL and GA. GA is an evolutionary computational method for solving optimization problems. It is one of the search methods that can rapidly find the optimal solution, as shown in Fig. 5 (Holland, 1975); (Holland,1992). This algorithm reflects the evolutionary process of

living organisms in its optimization process and consists of three distinctive methods: crossing, natural selection, and mutation. Crossing and natural selection can efficiently generate better parameter combinations. Furthermore, mutation enables the finding of the optimal solution for parameters that are far from the initial conditions (Takagi et al., 2023).

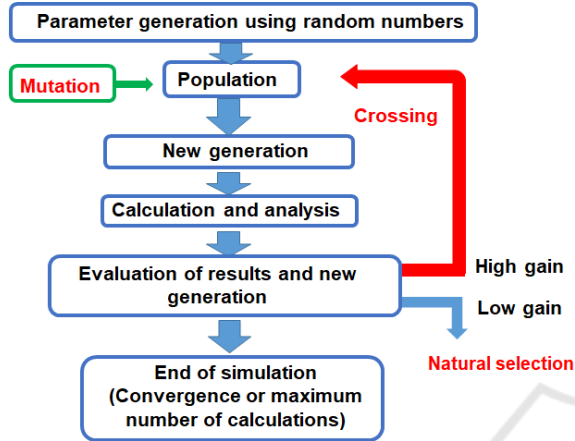


Figure 5: Optimization flow using GA.

The optimization software modeFRONTIER incorporating NSGA-II was used for GA calculations. NSGA-II is a GAs proposed by Debi et al. (Debi et al., 2022). It has excellent convergence and computational stability. Figure 6 shows the flow of the coupled calculation of modeFRONTIER and nextnano.QCL. Table 2 shows the calculation method and setting parameters. In this calculation, the gain and wavelength were extracted from the results of calculation using nextnano.QCL.

In the optimization, the parameter sets that maximize gains as the objective function were calculated. Furthermore, under the conditions where the wavelength was not in the range from 4.0 μm to 5.0 μm , we judged the parameter sets to be inappropriate. In the calculation using the GA, 10 parameter sets were calculated simultaneously as the same generation, and 10 new parameter sets in the next generation were created using the gain and wavelength as evaluation indicators. These calculation processes were repeated 100 times, and 1000 types of the parameter sets were calculated and evaluated.

The actual calculation was performed as follows. Referring to the film thicknesses in the QCL reported previously (Evans et al., 2007), each film thickness was determined using random numbers within the range of initial film thicknesses ± 1.0 nm. Ten parameter sets were generated and used for the first generation. The parameter sets were inputted into

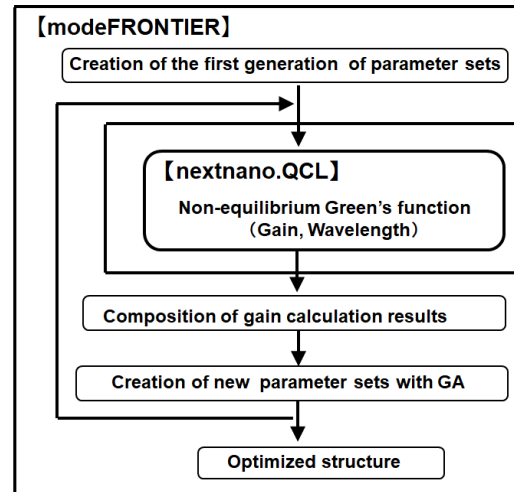


Figure 6: Coupled calculation of QCL and optimization simulators.

Table 2: Calculation method and setting parameters.

| Optimization method | GA (NSGA-II) |
|--|------------------|
| Objective functions | Gain, Wavelength |
| Number of parameter sets in N^{th} generation | 10 |
| Number of generations | 100 |
| Total number of simulations | 1000 |

nextnano.QCL in order and the gains and wavelengths were calculated. Among the calculation results, parameter sets with high gains were synthesized by taking the average film thickness (crossing). On the other hand, parameter sets with low gains were discarded (natural selection). In addition, a certain film thickness was randomly changed (mutation) in several parameter sets. Then, ten parameter sets were generated by crossing, natural selection, and mutation, and used as the second generation of parameter sets. By repeating the series of calculations up to 100th generation, we optimized nine film thicknesses in the active region.

4 SIMULATION RESULTS

Figure 7 shows the modeFRONTIER setting screen showing the flow of calculation. The upper row shows the input parameters, the middle row shows the nextnano.QCL calculation, and the lower row shows the output items. The input parameters correspond to the nine film thicknesses shown in Table 1. The nine film thicknesses of the injector barrier and active region were inputted into nextnano.QCL, and the gain and wavelength for each film structure were

calculated. On the basis of the gain, the next-generation parameter set was obtained using the GA described in Section 3.2, and the process of optimization proceeded.

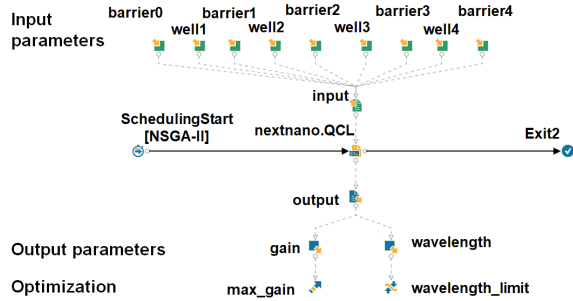


Figure 7: Setting screen of modeFRONTIER for optimization of active region in QCL.

To examine the effect of optimization by experiments, we added the reference structure reported previously (Evans et al., 2007) and the verification structure in which all film thicknesses were reduced by 10% to the optimization calculations. The reason for reducing the film thickness of each layer by -10% was that such a film can be deposited by shortened MBE process time and the desired film structure can be reliably produced.

Figure 8 shows the results of the coupled calculation of nextnano.QCL and genetic algorithm. The horizontal axis shows the number of calculation, and the vertical axis shows the gain of the structure corresponding to the calculation number. As the generation of genetic algorithms increases, the gain increases.

The reason why the gain intermittently decreases during optimization is that the mutation conditions for the GA were calculated and some of them showed low gains. As a result, while the gain of the reference structure was 50.01 cm^{-1} , that of the verification

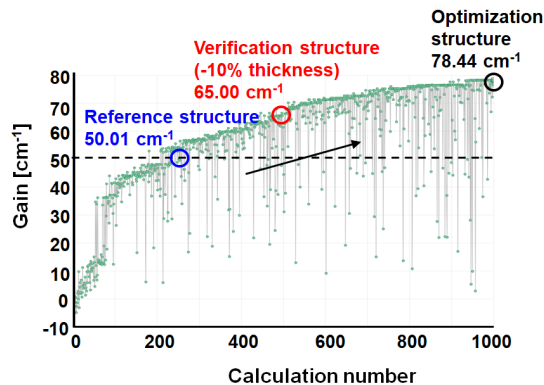


Figure 8: Progress in optimization by coupled calculation of genetic algorithm and QCL simulator.

structure was as high as 65.00 cm^{-1} . Furthermore, in the final structure, a gain of 78.44 cm^{-1} was obtained, and it was estimated that high-power laser oscillations can be obtained.

5 EVALUATION OF OPTIMIZATION RESULTS

To examine the validity of the optimization calculations, we fabricated prototype devices with the reference and verification structures, and we examined the EL light output. Figure 9(a) shows a photograph of external the prototype QCL chip. The injector and active regions, which contribute to light emission, were stacked 33 times, and the chip had a length of 2 mm and a ridge width of 100 μm .

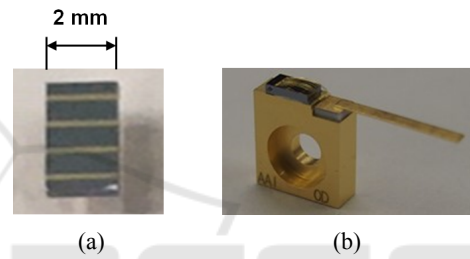


Figure 9: Photograph of prototype QCL. (a) QCL chip with length of 2 mm and ridge width of 100 μm , and (b) QCL device soldered on CuW mount.

Figure 9(b) shows a QCL device soldered on a CuW mount. The device was cooled to 77 K and operated at a frequency of 100 kHz and a pulse width of 300 nm (3% duty). The emitted light was focused by a concave mirror, and the EL intensity was measured by an MCT (HgCdTe) detector. Nicolet8700 (ThermoScientific Inc.) was used to measure the EL spectra.

Figure 10 shows the EL spectra of the prototype. The horizontal axis represents the wavelength and the vertical axis represents the EL emission intensity. A strong luminescence was observed for both the reference and verification structures. The oscillation wavelengths of the reference and verification structures were 4.53 μm and 4.77 μm , respectively. Here, in the simulation results in Section 4, the wavelengths of the reference and verification structures were 4.77 nm and 4.93 nm, respectively.

For both film structures, the experimental results had shorter wavelengths than the simulation results. However, in both experiments and simulations, the wavelengths of the verification structure were longer than those of the reference structure. The trend in the two types of structure was consistent in experiments

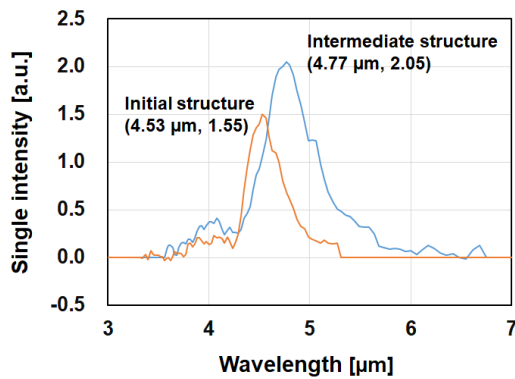


Figure 10: EL emission intensity of prototype QCL device (Tanimura et al., 2022).

and simulations. Corresponding to the gain of the optimization calculation, the emission intensity of the verification structure was 1.37 times higher than that of the reference structure. From these results, it is estimated that the structure optimized using the gain in the optimization simulation can have a higher emission intensity than the reference and verification structures.

6 CONCLUSIONS

We applied a coupled calculation of genetic algorithm and the QCLsimulator (nextnano.QCL) to calculate the gain that excites laser light in the active region of the QCL. The thicknesses of the nine layers constituting the active region were changed simultaneously, and the film structure with the maximum gain was determined from 1000 types of the parameter sets.

Nextnano.QCL incorporating a non-equilibrium Green's function was used to calculate the gain of QCL, and the validity of the simulation was evaluated using the active region structure reported previously (Evans et al., 2007). In the coupled calculation of genetic algorithm and nextnano.QCL, we used gain as an objective function and used the methods of crossing, natural selection, and mutation simulating the evolutionary process of living organisms to optimize the nine film thicknesses in the active region. As a result of the optimization calculation, the optimized structure had a gain (78.44 cm^{-1}) higher than that (50.01 cm^{-1}) in the structure reported in a previous paper.

In addition, as a result of prototyping the QCL of the reference and verification structures and measuring the EL emission, the emission intensity of 1.37 higher than that of the literature structure was

obtained for the verification structure, demonstrating the validity of the optimization.

ACKNOWLEDGEMENTS

This work was supported by Innovative Science and Technology Initiative for Security, ATLA, Japan.

REFERENCES

- Faist, J., Capasso F., Sivco D. L., Sirtori C., Hutchinson A. L., & Cho A. Y., 1994. "Quantum cascade laser", *Science*, 264, 553–556.
- Faist J., Villares G., Scalari G., Rösch M., Bonzon C., Hugi A., & Beck M., 2016. "Quantum Cascade Laser Frequency Combs", *Nanophotonics*, 5, 272–291.
- Lu S. L., Schrottke L., Teitsworth S. W., Hey R., & Grahn H. T., 2006. "Formation of electric-field domains in GaAs/AlxGal–xAs quantum cascade laser structures", *Phys. Rev. B*, 73, 033311.
- Grange, T., 2015. "Contrasting influence of charged impurities on transport and gain in terahertz quantum cascade lasers", *Phys. Rev. B*, 92, 241306-1–5.
- Tanimura H., Takagi S., Kakuno T., Hashimoto R., Kaneko K., & Saito S., 2022. "Analyses of Optical Gains and Oscillation Wavelengths for Quantum Cascade Lasers Using the Nonequilibrium Green's Function Method", *Journal of Computer Chemistry, Japan-International Edition*, 8, 2021–0024.
- Evans, A., Darvish, S. R., Slivken, S., Nguyen, J., Bai, Y., & Razeghi, M., 2007. "Buried heterostructure quantum cascade lasers with high continuous-wave wall plug efficiency", *Appl. Phys. Lett.* 91, 071101.
- Takagi S., Tanimura H., Kakuno T., Hashimoto R., & Saito S., 2021. "Evaluation of Simulator Incorporating Non-equilibrium Green's Function and Improvement of Quantum Cascade Lasers Output using the Simulator", *Proceedings of PHOTOPTICS 2021*, 58–63.
- Holland J. H., 1975. "Adaptation in natural and artificial systems: an introductory analysis with applications to biology, control, and artificial intelligence", University of Michigan Press.
- Holland J. H., 1992. "Genetic Algorithms", *Scientific American*, 267, 66–73.
- Takagi S., Sekine M., Nakaegawa T., & Hsiao S.-N., 2023. "Optimization of RF Frequencies in Dual-Frequency Capacitively Coupled Plasma Apparatus Using Genetic Algorithm (GA) and Plasma Simulation", *IEEE Trans. Semicond. Manuf.*, 36, 547–552.
- Debi K., Pratap A., Agarwal S., & Meyaraivan T., 2022. "A Fast and Elitist Multiobjective Genetic Algorithm: NSGA-II", *IEEE Trans. Comput.*, 6, 182–197.